Abstract for The 23^{rd} International Workshop on Water Waves and Floating Bodies, Jeju City, Korea, April 13-16, 2008.

Interference Drag of Multiple Pressure Cushions

Ronald W. Yeung¶, Hui Wan, and Jae-Moon Lew*
Department of Mechanical Engineering
University of California at Berkeley, Berkeley, CA 94720-1740, USA
¶Correspondence author. E-mails: *rwyeung@berkeley.edu*, *wanh@berkeley.edu*, & *jmlew@cnu.ac.kr*

1 Background

Faster speed, yet lower power consumption, has often been the design objective of high-performance marine vehicles such as hovercrafts, Surface-Effect Ships (SES), among others. Lower power consumption also means less carbon-dioxide emission, an issue of great environmental concern. The concept of a multi-hull system offers favorable possibility of powering reduction in steady motion. Configuration arrangement of component hulls is therefore an important design issue to address.

The problems of steady forward-motion of multi-hulls and SES (hulls with a pressure cushion) were analyzed in Yeung et al. [1], and Yeung & Wan [2], respectively. Therein, linearized theory was used to obtain the interference wave resistance, which can be either positive or negative, increasing or reducing the powering for a given speed. Results for a single pressure cushion are quite well known (see, e.g., Wehausen & Laitone [3], Newman & Poole [4], and Doctors & Sharma [5]). The possibility of shaping the pressure function within a cushion was considered in the interesting work of Tuck et al. [6]. However, the effects of combining multiple numbers of cushions, perhaps even of dis-similar shapes, have yet to be thoroughly explored. This paper addresses the multiple pressure-cushion problem in the same vein as [1] & [2], with the aim of obtaining the necessary interference expressions for rapid evaluation of the behavior of a pressure collection. Given that there have been reports [7] on the use of multiple cushions to successfully improve the rides and maneuverability of SES and other cushioned crafts, developing a methodology to assess the powering performance of multi-cushions is desirable.

2 Resistance of a Translating Pressure Cushion

Within the framework of linear theory, the generalized steady wave resistance problem can be summarized as finding a velocity potential $\phi(x,y,z)$ that satisfies Laplace's equation, but is subject to the free-surface boundary condition:

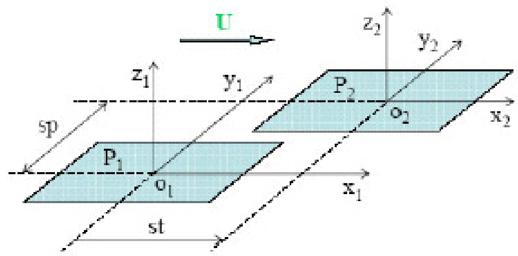

Figure 1: *Coordinate systems: shown for two pressure cushions with separation and stagger.*

$$k_0\phi_z(x,y,0)+\phi_{xx}(x,y,0)=P_x(x,y)/\rho U \tag{1}$$

where $k_0 = g/U^2$ and U is the forward speed in direction x (Fig. 1) and ρ the water density. Here, $P(x,y)$ is the applied (cushion) pressure, which vanishes except in the planform regions S_P. Conditions of decaying disturbances as $z\to-\infty$ and the absence of upstream waves ($x\to\infty$) are also to be observed. We note also that the linearized fluid pressure p and the longitudinal free-surface slope ζ_x are given by:

$$p(x,y,z)-P(x,y) = -\rho U\phi_x + \rho g z, \tag{2}$$
$$g\zeta_x(x,y) = U\phi_{xx}(x,y,0) - P_x/\rho. \tag{3}$$

The velocity potential $\phi_P(x,y,z)$ can be given in terms of derivative of the Green function G as:

$$\phi_P = \frac{U}{4\pi\rho g}\iint_{S_P} P(\xi,\eta)G_x(x-\xi;y-\eta;z,0)d\xi d\eta\ , \tag{4}$$

after performing an integration by part in ξ. The Green function G is given in [3]:

$$\begin{aligned}G(x-\xi;y-\eta;z,\zeta) &= -\frac{1}{r}+\frac{1}{r_1}+\frac{4k_0}{\pi}\int_0^{\pi/2} d\theta\sec^2\theta \\ &\int_0^{\infty} dk\frac{e^{k(z+\zeta)}}{k-k_0\sec^2\theta}\cos[k(x-\xi)\cos\theta]\cos[k(y-\eta)\sin\theta] \\ &+4k_0\int_0^{\pi/2} d\theta\sec^2\theta e^{k_0(z+\zeta)\sec^2\theta}\sin[k_0(x-\xi)\sec\theta] \\ &\times\cos[k_0(y-\eta)\sin\theta\sec^2\theta] \\ &\equiv G_L+G_w\end{aligned} \tag{5}$$

*Visiting Scholar: Dept. of Naval Arch. & Marine Engrg., Chungnam National University, Taejon 305-764, Korea where G_L and G_w denote the terms that are symmetric (the first three) and asymmetric with respect to $(x-\xi)$, respectively.

The wave resistance induced by a moving cushion is given by the integral of product of the pressure P and free-surface slope Eq. (3): $-\iint_{S_P} P(x,y)\zeta_x d\xi d\eta$ and can be simplified to (with the change of variable $\lambda = \sec\theta$):

$$R_{wP} = \pi\rho U^2 \int_1^\infty \frac{d\lambda}{\lambda^4\sqrt{\lambda^2-1}} |A_P(\lambda)|^2, \quad (6)$$

where $A_P(\lambda)$, the complex wave-making amplitude (or the Kochin) function, is given by :

$$A_P(\lambda) = \frac{k_0\lambda^4}{\pi\rho U^2} \iint_{S_P} P(\xi,\eta) e^{ik_0\lambda(\xi+\sqrt{\lambda^2-1}\eta)} d\xi d\eta \quad (7)$$

In arriving at Eq. (6), we note that there was no contribution from G_L. Further, from Eqs. (6-7), we observe that R_{wP} will be decreased by 75% when pressure P is reduced by 50%. So, smaller P is favored in terms of reducing wave resistance. However this will increase the size of the cushion for a fixed displacement.

A pressure cushion profile of peak value P_m that is infinitely differentiable in the horizontal plane [4] is shown in Fig. 2. This hyperbolic tangent form with the tapering parameters α and β, in the longitudinal and transverse directions respectively, leads to a closed form expression for (7) (see [2]).

For a confirmation of our computed results with

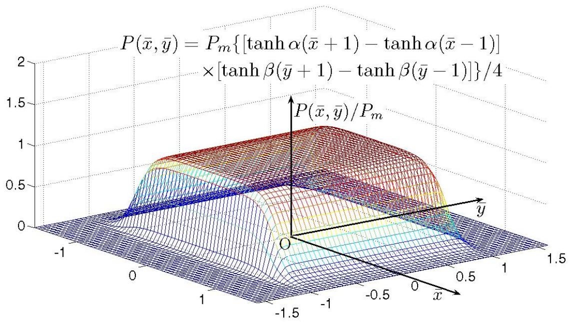

Figure 2: *Pressure function $P(x,y)$ of a cushion (α=5, β=20) in unitized variables: $\overline{x} = 2x/B_p$, $\overline{y} = 2y/L_p$.*

[4], the wave resistance experienced by the pressure cushion is shown in Fig. 3 as a function of the Froude number (F_n^{-2}), with the beam-to-length ratio, B_P/L_P, of the cushion as a parameter. Here, the non-dimensionalized resistance coefficient is defined by

$$C_{wP} = \frac{R_{wP}}{2P_m^2 B_P/\rho g} \propto \frac{R_{wP}}{2\Delta(h/L_P)}, \quad (8)$$

where Δ is the displacement (or "lift") due to the cushion, and h/L_P is the (hydrostatic) head of P_m to cushion length L_P ratio. The plot provides the interesting observation: The wave drag to displacement ratio is proportional to the head-to-length ratio times a function that depends only on B_P/L_P and F_n. In Fig. 3,for a fixed h/L_P, a wide cushion always yields higher resistance. The highly oscillatory behavior is related to the interference of the waves generated by the bow and stern of the cushion.

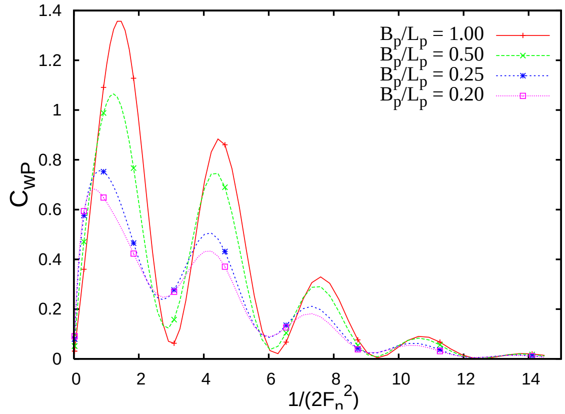

Figure 3: *C_{wP} for a rectangular cushion,* α=5, β=20.

3 Dual Cushions with Separation and Stagger

In the case of two pressure cushions with separation and stagger, as defined in Fig. 1, the total wave resistance R_{wT} on the two pressure cushions is not only the sum of the resistance due to pressure $P_1(x,y)$ (i.e., R_{wP_1}) and pressure P_2 (R_{wP_2}) individually, but also of an interference term $R_{wP_1 \rightleftarrows P_2}$, which cannot be ignored. This term accounts for the effect of pressure 1 on pressure 2 ($R_{wP_1\to P_2}$) as well as the effect of pressure 2 on pressure 1 ($R_{wP_1\leftarrow P_2}$), or effectively, the superposition of the wave-interference effects of each of the surface distribution in the field. Following [1], we can establish:

$$\begin{aligned} R_{wT} &= R_{wP_1} + R_{wP_2} + R_{wP_1\rightleftarrows P_2} \\ &= R_{wP_1} + R_{wP_2} + R_{wP_1\to P_2} + R_{wP_1\leftarrow P_2} \quad (9) \end{aligned}$$

where R_{wP_1} and R_{wP_2} are each given by the equivalents of the Michell formula [8], or Eq. (6-7) here.

3.1 The Interference Resistance $R_{wP_1\rightleftarrows P_2}$

Consider the two local frames of reference, $O_1x_1y_1z_1$ and $O_2x_2y_2z_2$ in Fig.1. Using Eqs. (2-4), we can write the expression of the interference resistances $R_{wP_1\to P_2}$ (pressure 2 acting on the wave slope at cushion 2 generated by cushion 1) and $R_{wP_2\to P_1}$ (pressure 1 acting on the wave slope at cushion 1 generated by cushion 2) as:

$$R_{wP_1 \to P_2} = \frac{U^2}{4\pi\rho g^2} \iint_{S_{P_2}} P_2(x_2, y_2) dx_2 dy_2 \iint_{S_{P_1}} P_1(\xi_1, \eta_1) G_{x_2 x_2 x_2}(x_2 + st - \xi_1; y_2 + sp - \eta_1; z_2, 0) d\xi_1 d\eta_1 \quad (10)$$

$$R_{wP_2 \to P_1} = \frac{U^2}{4\pi\rho g^2} \iint_{S_{P_1}} P_1(x_1, y_1) dx_1 dy_1 \iint_{S_{P_2}} P_2(\xi_2, \eta_2) G_{x_1 x_1 x_1}(x_1 - st - \xi_2; y_1 - sp - \eta_2; z_1, 0) d\xi_2 d\eta_2 \quad (11)$$

Then combining Eqs. (10) and (11), and recalling that $x_2 = x_1 - st,\ y_2 = y_1 - sp$, and $z_2 = z_1$, we can show that the *summed* resistance on the two pressure cushions can be written as:

$$R_{wP_1 \rightleftharpoons P_2} = \frac{-U^2}{2\pi\rho g^2} \iint_{S_{P_1}} P_1(x_1, y_1) dx_1 dy_1 \iint_{S_{P_2}} P_2(\xi_2, \eta_2) G_{w x_1 x_1 x_1}(x_1 - st - \xi_2; y_1 - sp - \eta_2; 0, 0) d\xi_2 d\eta_2 \quad (12)$$

Of interest is that only G_w survives in this summation. Eq. (12) is still unwieldy. However, if *both* cushions are symmetric about their own x axis, $P(x, -y) = P(x, y)$, the result simplifies greatly in a manner similar to the hull-to-hull interference problem of [1]. Under this assumption, A_P in Eq. (7) can be written as:

$$A_P(\lambda) = \frac{k_0 \lambda^4}{\pi\rho U^2} \iint_{S_P} P(\xi, \eta) e^{i k_0 \lambda \xi} \cos(k_0 \lambda \sqrt{\lambda^2 - 1}\eta) d\xi d\eta \quad (13)$$

and the interference resistance is given by:

$$R_{wP_1 \rightleftharpoons P_2} = 2\pi\rho U^2 \int_1^\infty \frac{d\lambda}{\lambda^4 \sqrt{\lambda^2 - 1}} \cos(k_0 sp \lambda \sqrt{\lambda^2 - 1}) \times \{\Re(A_{P_1} \bar{A}_{P_2}) \cos(k_0 \lambda st) + \Im(A_{P_1} \bar{A}_{P_2}) \sin(k_0 \lambda st)\} \quad (14)$$

Here, $\Re$ and $\Im$ denote real and imaginary parts, respectively. Similarly, if the pressure cushions have symmetry about the y axis, $P(x, y) = P(-x, y)$, i.e. fore-aft symmetry, then Eq. (7) can be written as:

$$A_P(\lambda) = \frac{k_0 \lambda^4}{\pi\rho U^2} \iint_{S_P} P(\xi, \eta) e^{i k_0 \lambda \sqrt{\lambda^2 - 1}\eta} \cos(k_0 \lambda \xi) d\xi d\eta, \quad (15)$$

and the interference resistance will be:

$$R_{wP_1 \rightleftharpoons P_2} = 2\pi\rho U^2 \int_1^\infty \frac{d\lambda}{\lambda^4 \sqrt{\lambda^2 - 1}} \cos(k_0 \lambda st) \times \{\Re(A_{P_1} \bar{A}_{P_2}) \cos(k_0 \lambda \sqrt{\lambda^2 - 1} sp) + \Im(A_{P_1} \bar{A}_{P_2}) \sin(k_0 \lambda \sqrt{\lambda^2 - 1} sp)\} \quad (16)$$

Eqs. (14) and (16) show explicitly how the staggerand separation between the pressure cushions can influence the total wave resistance. These new expressions can be computed concurrently with the mono-pressure resistances $R_{wj}, j = 1, 2$, given by Eq. (6).

4 Results and Discussion

Restricting the investigation to dual cushions in this paper, we show some sample results of having first dual cushions in parallel, and then in tandem, configurations. For $B_P/L_P = 0.5$, we compare the performance of the dual cushions, each of peak pressure P_m, against a mono-cushion of the same displacement and geometry. The mono-cushion resistance R_0, therefore, has a pressure of $2P_m$, applied over the same "footprint". Figs. 4 and 5 show the interference and total wave resistance, respectively, relative to R_0 for dual cushions in a parallel configuration. In these figures, the surface functions approach unity at $sp = 0$, when the two cushions overlay. Then both functions drop off in an oscillatory manner in both directions. Significant interference drag occurs when sp/B_p is $\sim$ unity and F_n is below the first resistance hollow of the mono-cushion. Note that for large F_n or sp, the dual-cushion resistance approaches the expected value of 50% of that of the mono-cushion.

To obtain the actual dual-cushion C_{wT}, one should multiply the R_T/R_0 ratio by C_o, the mono-cushion resistance coefficient defined by Eq. (8), this latter function is plotted as a *trace* against F_n for reference.

The corresponding results of having the dual cushions in tandem with st being varied are shown in Figs. 6 and 7. The oscillatory patterns are more complex. The lower F_n region shows clearly the interefer-ence effects of transverse waves. Besides that, a valley of low total drag occurs for a combination of F_n and st/L_p. This valley extends to larger values of st/L_p (partly visible).

The effects of varying both stagger and separation are shown in Figs. 8 and 9 for $F_n = 0.42$, which is at the first hollow, and for a higher Froude number, $F_n = 1$. Here, λ_o is the maximum (transverse) wavelength of the Kelvin wave system. These plots parallel the so-called Weinblum configurations of di-hulls. The behavior at the two speeds are drastically different, but R_T/R_o at 30% is achievable for a wide range of sp–st combinations. These and other complex features will be further discussed in the Workshop.

REFERENCES

1. Yeung, R.W., Poupard, G. and Toilliez,J.O., *SNAME Trans.*, Vol.112, 2004, pp. 142–169.
2. Yeung, R.W., H. Wan, *ASME J. Offsh Mech & Arctic Engrg*, 2008, in press.
3. Wehausen, J. V. and Laitone, E. V., *Handbuch der Physik*, Vol. 9, Springer-Verlag, Berlin, 1960,
4. Newman,J.N. and Poole, F.A.P., *Shiffstechnik*, Bd. 9, Heft 45, 1962, pp. 21-26.
5. Doctors, L.J. and Sharma, S.D., *J. Ship Res*, Vol. 16, 1972, pp. 248-260
6. Tuck, E. O., Scullen, D.,and Lazauskas, L., *Proc.* 24^{th} *Symp. Naval Hydrodyn.* , Fukuoka, Japan, 2002.
7. Burg, Donald E., "Multiple Cushion Air-Ride Boat Hull", WIPO Patent: WO/1992/013753, 1992.
8. Michell, J.H., *Philosophical Magazine*, Ser. 5, Vol. 45, 1898, pp. 106-123.

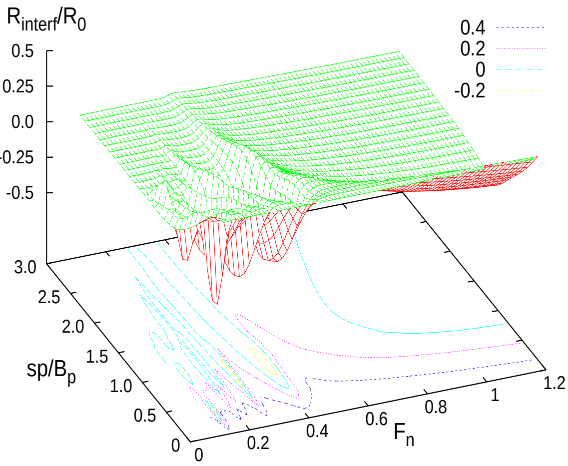

Figure 4: R_{interf}/R_0 *for dual cushions vs.* F_n *and* sp*, for* $st = 0$.

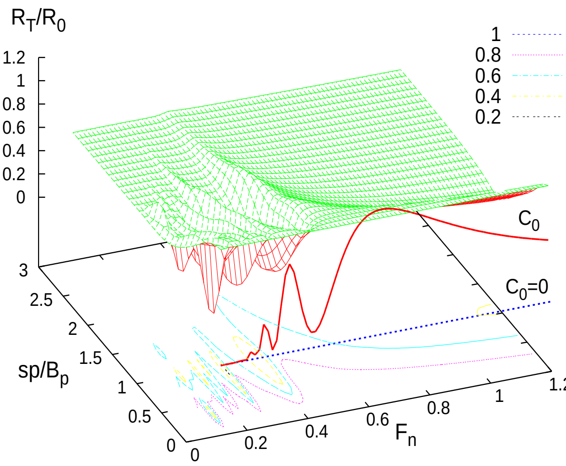

Figure 5: R_T/R_0 *vs.* F_n *and* sp*, for* $st = 0$*, with* $C_0(F_n)$ *shown.*

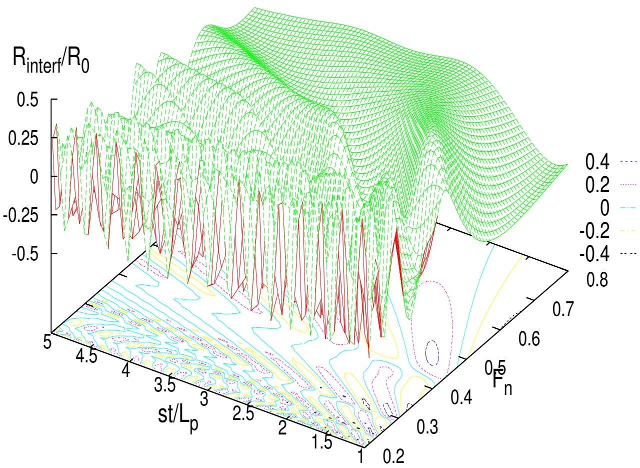

Figure 6: R_{interf}/R_0 *vs.* F_n *and* st *for dual cushions in tandem* $(sp = 0)$.

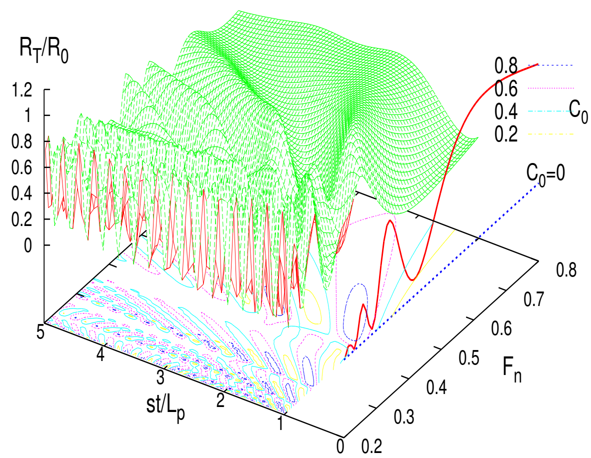

Figure 7: R_T/R_0 *vs.* F_n *and* st*, for dual cushions in tandem* $(sp = 0.)$*, with* $C_0(F_n)$ *shown.*

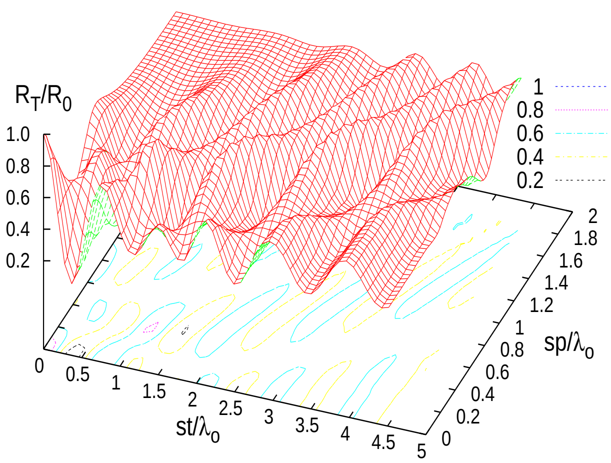

Figure 8: *Dual-cushion* R_T/R_0 *vs.* st/λ_o *and* sp/λ_o*, at* $F_n = 0.42$

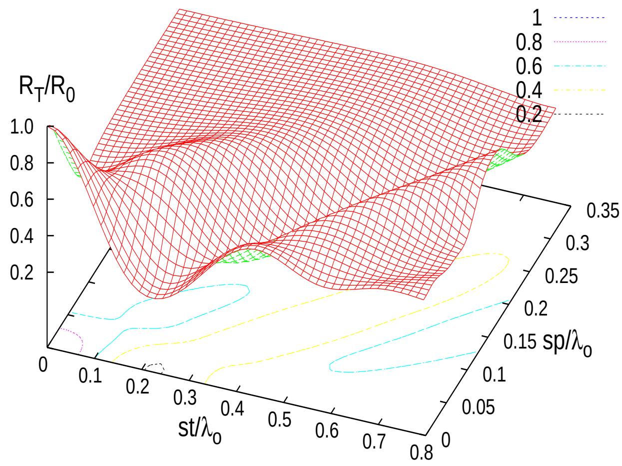

Figure 9: *Dual-cushion* R_T/R_0 *vs.* st/λ_o *and* sp/λ_o*, at* $F_n = 1.0$